Biomedical Optics EXPRESS

Development of a luminous textile for reflective pulse oximetry measurements

Marek Krehel,[1,2] Martin Wolf,[3] Luciano F. Boesel,[1,*] René M. Rossi,[1] Gian-Luca Bona,[1,2] and Lukas J. Scherer[1]

[1]*Empa, Swiss Federal Laboratories for Materials Science and Technology, Laboratory for Protection and Physiology, Lerchenfeldstrasse 5, St. Gallen 9014, Switzerland*
[2]*ETH Zurich, Swiss Federal Institute of Technology, Department of Information Technology and Electrical Engineering, Gloriastrasse 35, Zurich 8092, Switzerland*
[3]*Biomedical Optics Research Laboratory, Clinic of Neonatology, University Hospital Zurich, Frauenklinikstrasse 10, 8091 Zurich, Switzerland*
**Luciano.Boesel@empa.ch*

Abstract: In this paper, a textile-based sensing principle for long term photopletysmography (PPG) monitoring is presented. Optical fibers were embroidered into textiles such that out-coupling and in-coupling of light was possible. The "light-in light-out" properties of the textile enabled the spectroscopic characterization of human tissue. For the optimization of the textile sensor, three different carrier fabrics and different fiber modifications were compared. The sample with best light coupling efficiency was successfully used to measure heart rate and SpO2 values of a subject. The latter was determined by using a modified Beer-Lambert law and measuring the light attenuation at two different wavelengths (632 nm and 894 nm). Moreover, the system was adapted to work in reflection mode which makes the sensor more versatile. The measurements were additionally compared with commercially available system and showed good correlation.

OCIS codes: (060.2310) Fiber optics; (060.2370) Fiber optics sensors.

References and links

1. J. W. Zheng, Z. B. Zhang, T. H. Wu, and Y. Zhang, "A wearable mobihealth care system supporting real-time diagnosis and alarm," Med. Biol. Eng. Comput. **45**(9), 877–885 (2007).
2. C. N. Scanaill, S. Carew, P. Barralon, N. Noury, D. Lyons, and G. M. Lyons, "A review of approaches to mobility telemonitoring of the elderly in their living environment," Ann. Biomed. Eng. **34**(4), 547–563 (2006).
3. E. R. Post, M. Orth, P. R. Russo, and N. Gershenfeld, "E-broidery: Design and fabrication of textile-based computing," IBM Syst. J. **39**(3.4), 840–860 (2000).
4. O. Ziemann, J. Krauser, P. E. Zamzow, and W. Daum, *POF-Handbook* (Springer, Berlin, 2008).
5. M. G. Kuzyk, "Polymer Fiber Optics," (2007), pp. 97–98.
6. T. Pola and J. Vanhala, "Textile electrodes in ECG measurement," Proceedings of the 2007 International Conference on Intelligent Sensors, Sensor Networks and Information Processing, 635–639 (2007).
7. M. Krehel, R. M. Rossi, G. L. Bona, and L. J. Scherer, "Characterization of Flexible Copolymer Optical Fibers for Force Sensing Applications," Sensors (Basel) **13**(9), 11956–11968 (2013).
8. B. Selm, E. A. Gurel, M. Rothmaier, R. M. Rossi, and L. J. Scherer, "Polymeric Optical Fiber Fabrics for Illumination and Sensorial Applications in Textiles," J. Intell. Mater. Syst. Struct. **21**(11), 1061–1071 (2010).
9. M. Rothmaier, B. Selm, S. Spichtig, D. Haensse, and M. Wolf, "Photonic textiles for pulse oximetry," Opt. Express **16**(17), 12973–12986 (2008).
10. C. Balas, "Review of biomedical optical imaging-a powerful, non-invasive, non-ionizing technology for improving in vivo diagnosis," Meas. Sci. Technol. **20**(10), 104020 (2009).
11. F. Narbonneau, D. Kinet, B. Paquet, A. Depré, J. de Jonckheere, R. Logier, J. Zinke, J. Witt, and K. Krebber, "Smart Textile Embedding Optical Fiber Sensors for Healthcare Monitoring during MRI," Adv. Sci. Technol. **60**, 134–143 (2008).
12. T. G. Giallorenzi, J. A. Bucaro, A. Dandridge, G. H. Sigel, J. H. Cole, S. C. Rashleigh, and R. G. Priest, "Optical Fiber Sensor Technology," IEEE J. Quantum Electron. **18**(4), 626–665 (1982).
13. S. Liehr, P. Lenke, M. Wendt, K. Krebber, M. Seeger, E. Thiele, H. Metschies, B. Gebreselassie, and J. C. Munich, "Polymer Optical Fiber Sensors for Distributed Strain Measurement and Application in Structural Health Monitoring," IEEE Sens. J. **9**(11), 1330–1338 (2009).
14. J. Y. Ding, M. R. Shahriari, and G. H. Sigel, "Fiber Optic Ph Sensors Prepared by Sol-Gel Immobilization Technique," Electron. Lett. **27**(17), 1560–1562 (1991).

#211135 - $15.00 USD Received 29 Apr 2014; revised 7 Jun 2014; accepted 8 Jun 2014; published 9 Jul 2014

15. J. Witt, F. Narbonneau, M. Schukar, K. Krebber, J. De Jonckheere, M. Jeanne, D. Kinet, B. Paquet, A. Depré, L. T. D'Angelo, T. Thiel, and R. Logier, "Medical textiles with embedded fiber optic sensors for monitoring of respiratory movement," IEEE Sens. J. **12**(1), 246–254 (2012).
16. J. Rantala, J. Hannikainen, and J. Vanhala, "Fiber optic sensors for wearable applications," Pers. Ubiquitous Comput. **15**(1), 85–96 (2011).
17. E. Hanada, "The electromagnetic environment of hospitals: how it is affected by the strength of electromagnetic fields generated both inside and outside the hospital," Ann. Ist. Super. Sanita **43**(3), 208–217 (2007).
18. R. F. Edlich, K. L. Winters, C. R. Woodard, R. M. Buschbacher, W. B. Long, J. H. Gebhart, and E. K. Ma, "Pressure ulcer prevention," J. Long Term Eff. Med. Implants **14**(4), 285–304 (2004).
19. R. Woodgate and L. J. Kristjanson, "A young child's pain: How parents and nurses 'take care'," Int. J. Nurs. Stud. **33**(3), 271–284 (1996).
20. S. L. J. R. Hufenus, D. Hegemann, F. A. Reifler, and S. Gaan, "Developing base technologies for tomorrow's smart textiles," 18th International conference on composite materials (2011).
21. B. Toth, A. Becker, and B. Seelbach-Göbel, "Oxygen saturation in healthy newborn infants immediately after birth measured by pulse oximetry," Arch. Gynecol. Obstet. **266**(2), 105–107 (2002).
22. A. T. Rheineck-Leyssius and C. J. Kalkman, "Influence of pulse oximeter settings on the frequency of alarms and detection of hypoxemia: Theoretical effects of artifact rejection, alarm delay, averaging, median filtering or a lower setting of the alarm limit," J. Clin. Monit. Comput. **14**(3), 151–156 (1998).
23. J. P. Isbister, "Physiology and pathophysiology of blood volume regulation," Transfus. Sci. **18**(3), 409–423 (1997).
24. B. Venema, N. Blanik, V. Blazek, H. Gehring, A. Opp, and S. Leonhardt, "Advances in reflective oxygen saturation monitoring with a novel in-ear sensor system: Results of a human hypoxia study," IEEE Trans. Biomed. Eng. **59**(7), 2003–2010 (2012).
25. E. K. Svanberg, P. Wollmer, S. Andersson-Engels, and J. Akeson, "Physiological influence of basic perturbations assessed by non-invasive optical techniques in humans," Br. J. Anaesth. **108**, 272–273 (2012).
26. U. Wolf, M. Wolf, J. H. Choi, M. Levi, D. Choudhury, S. Hull, D. Coussirat, L. A. Paunescu, L. P. Safonova, A. Michalos, W. W. Mantulin, and E. Gratton, "Localized irregularities in hemoglobin flow and oxygenation in calf muscle in patients with peripheral vascular disease detected with near-infrared spectrophotometry," J. Vasc. Surg. **37**(5), 1017–1026 (2003).
27. U. Wolf, M. Wolf, J. H. Choi, L. A. Paunescu, A. Michalos, and E. Gratton, "Regional differences of Hemodynamics and oxygenation in the human calf muscle detected with near-infrared spectrophotometry," J. Vasc. Interv. Radiol. **18**(9), 1094–1101 (2007).
28. A. C. M. Dassel, R. Graaff, A. Meijer, W. G. Zijlstra, and J. G. Aarnoudse, "Reflectance pulse oximetry at the forehead of newborns: The influence of varying pressure on the probe," J. Clin. Monit. **12**(6), 421–428 (1996).
29. N. A. A. Rahim, W. McDaniel, K. Bardon, S. Srinivasan, V. Vickerman, P. T. C. So, and J. H. Moon, "Conjugated Polymer Nanoparticles for Two-Photon Imaging of Endothelial Cells in a Tissue Model," Adv. Mater. **21**(34), 3492–3496 (2009).
30. A. Louw, C. Cracco, C. Cerf, A. Harf, P. Duvaldestin, F. Lemaire, and L. Brochard, "Accuracy of pulse oximetry in the intensive care unit," Intensive Care Med. **27**(10), 1606–1613 (2001).

1. Introduction

Due to the aging society, medical textiles are attracting more attention every day. In the next decades, wearable sensors are expected to conduct continued and autonomous monitoring of life-sustaining parameters [1–3]. Different approaches of long-term body monitoring solutions using textile fabrics have been intensively studied in recent years [4, 5]. The electronics involved in the proposed solutions often influence the haptic of medical textiles negatively. To overcome that problem, flexible and smart fibers allow the separation of the rigid electronics from the measured region and thus from the body. Electrocardiography (ECG) is a well-documented example where very flexible electro-conductive yarns replaced rigid electrodes and therefore allowed long-term ECG monitoring [6].

Different research groups were attracted by the integration of polymer optical fibers into fabrics for different purposes [7–9]. In the medtech sector, luminous textiles have been reported to find applications as illuminating source in phototherapies or photodynamic therapies [8] or for sensing purposes [9]. Different ways to laterally out-couple light have been reported [8, 9]. The light out-coupling can be achieved by damaging the fiber surface [9], or by bending the fibers [3]. Moreover, the use of light-emitting diodes (LEDs) as light source provides low power consumption and long lifetime. The separation of the electronics from the body and the low power consumption makes luminous textiles ideal candidates for biomedical monitoring systems [10]. Other advantages of textile-integrated flexible optical fibers for wearable systems are the light-weight structure, insensitivity to electromagnetic fields, water and corrosion resistance, comfort, ease of movements, and reduced movement artefacts [8, 11–13]. Due to these benefits, optical fiber based sensors are used in numerous

#211135 - $15.00 USD Received 29 Apr 2014; revised 7 Jun 2014; accepted 8 Jun 2014; published 9 Jul 2014

applications to detect chemical or physical changes [9, 12, 14–16]. Insensitivity to electrical fields is of great importance, especially in hospitals where a lot of electromagnetic fields are present [17]. The combination of enhanced comfort while wearing the textiles and the resistance to above-mentioned parameters make photonic textiles practical for long-term monitoring systems of human vital parameters. Long term monitoring systems with enhanced haptic is very significant in monitoring paraplegic patients since any type of rigid sensors is a danger of causing decubitus ulcers [18]. The other planned application of the proposed textile-based SpO2 system is the monitoring of neonates to prevent psychological discomfort of parents caused by the big amount of medical apparatus [19]. To implement optical fibers into textiles, the fibers should be highly flexible, which is neither the case for glass-based nor for commercial available polymer optical fibers (POFs) made of polymethyl methacrylate (PMMA). For textile applications, there is a demand for polymer optical fibers made of more flexible polymers [8]. We have recently demonstrated that cyclo-olefin polymers are ideally suited for the production of flexible optical fibers [20]. As has been demonstrated in this study, these fibers withstand even strong mechanical stresses occurring during the industrial embroidering process. The mentioned SpO2 is a parameter that measures arterial oxygen saturation indirectly and non-invasively by means of measuring light absorption in human blood [21]. Monitoring of oxygen saturation is crucial since the delivery of oxygen to human organs is essential to prevent hypoxemia and maintaining humans in wellbeing [22]. The other application where a wearable SpO2 system in reflective mode is desired is for people performing high-altitude activities e.g. mountaineering or climbing. During this activities *hypothermia, trauma* or severe stress levels can occur. Since the blood perfusion of the extremities can be strongly decreased in this conditions, SpO2 measurements in transmission mode is no longer possible in the body extremities *e.g.* in the fingers [23–25]. The above mentioned solutions work either as rigid electronics that works in both modes (transmission and reflection) or as a flexible textile but only in transmission mode. So far no-one has reported SpO2 sensing textile that would work in reflection mode. In reflection mode, the working principle is the statistical fact that the further away the light is collected from the illumination point, the deeper the light has penetrated into the tissue, which allows the volumetric determination of the blood perfusion (photopletysmography) [26, 27].

In this study, we report on a proof of concept where optical fibers embroidered into textiles measured heart rate and oxygen saturation in the reflection mode. In contrast to transmission mode, the reflection mode is more versatile. It does not limit the measurements to places like fingertips, ear lobes or toes and enables the development of a wide variety of wearable sensing systems like T-shirts, hats, breast-belts, or armbands [28]. The results we achieved were cross compared with a commercial available and calibrated device. Moreover, we show that the integration of optical fibers in form of concentric rings enable the collection of light with constant distance from the light source as schematically presented in Fig. 1.

#211135 - $15.00 USD Received 29 Apr 2014; revised 7 Jun 2014; accepted 8 Jun 2014; published 9 Jul 2014

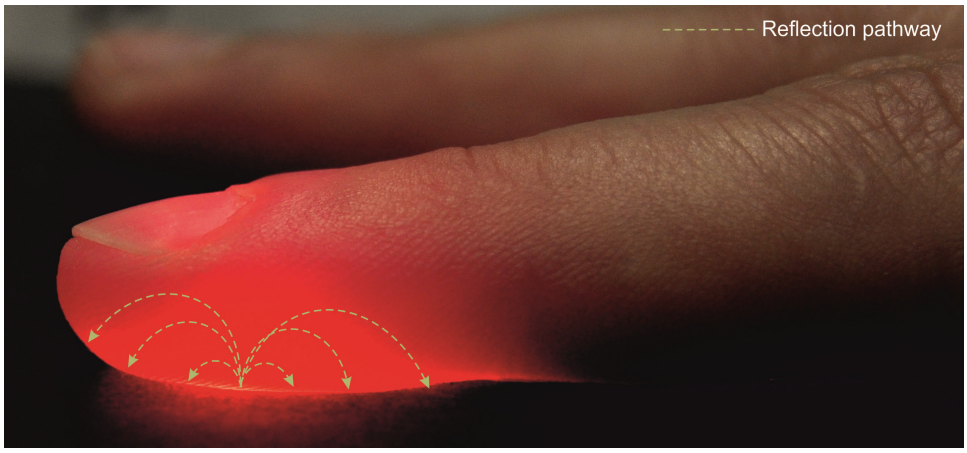

Fig. 1. Analysis of different depths of tissue. The further from the illumination point the deeper parts of tissue are penetrated (dotted line)

2. Materials and methods

2.1 Fiber type

The optical fibers used in this study were produced using a melt-spinning process. The core of the optical fibers was made of cycloolefin polymer, (Zeonor 1020R, Zeon, Düsseldorf, Germany) and as cladding material a fluorinated polymer (THVP 2030GX, Dyneon, Burgkirchen, Germany) was used. Refractive indices of the core and cladding are 1.53 and 1.35 respectively which gives numerical aperture (NA) of 0.72. The total diameter of the fibers was 152 µm with cladding thickness of 12 µm. Light attenuation of the optical fiber was 9 dB/cm at 652 nm, measured with the cut back method. Further details for the production of the optical fibers are found in [4].

2.2 Sample preparation

In Fig. 2, a sketch presenting the scheme of the stitching pattern with the optical fibers is illustrated. Between the optical fibers stitched in the middle (acting as light source) and the three embroidered rings (acting as a light collector), a three dimensional ring was embroidered with black polyester yarn provided by Schweninger Textil GmbH & CoKG (Lustenau, Austria)

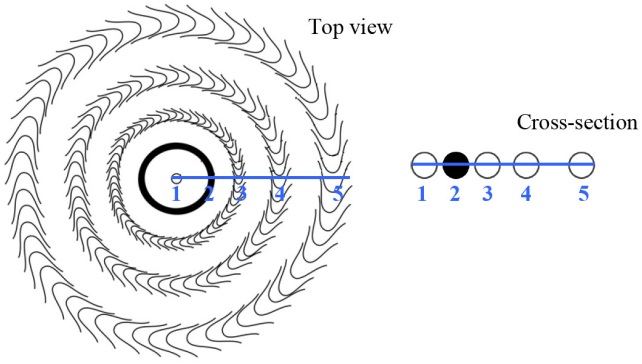

Fig. 2. Sketch presenting embroidered optical fibers. Where (1) optical fibers stitched to couple the light out; (2) three dimensional embroidered black ring to prevent light short circuit. (3),(4) and (5) represent rings of optical fibers stitched to couple the light in. Each “V”-shaped line in the rings represents a portion of a single optical fiber.

#211135 - $15.00 USD Received 29 Apr 2014; revised 7 Jun 2014; accepted 8 Jun 2014; published 9 Jul 2014

All the samples were produced at Forster Rohner AG (St. Gallen, Switzerland). The optical yarn was embroidered on the fabric using an embroidery machine ERA TM 0625 (Saurer AG, Switzerland). The carrier fabric was mounted on the vertical frame (1.60 m in width) whose movements corresponded to a digitalized embroidery pattern. In front of the fabric a perpendicularly positioned set of needles (type 4 RS/SPI nr "3770120137" manufactured by Bachmann AG Swiss) was threaded with the monofilament optical fiber. To obtain embroidery of a high quality the thread was pulled through the positive thread feed system, so called ActiFeed, that applied a tension of 85 g. The shuttle guide was positioned behind and parallel to the fabric, and at the height of the needles. The shuttle was threaded with polyester yarn (type, 80/2 Polyester (PES), white). Figure 3 shows two patterns of laying the optical yarn on the fabric surface ("M" and "V" type). Each line represents a portion of the laid optical yarn whereas red dots correspond to the points where the needle went through the fabric and interlaced optical yarn with the polyester yarn carried by shuttle. The zigzag stitch was used to create both patterns (Fig. 3) and optical yarn was laid on the face of the fabric whereas polyester yarn stayed at the opposite side of the fabric.

As carrier fabrics on which the embroidery was produced, three different types were tested: one thin woven, and one thin and one thick (70 g/m2 and 140 g/m2) nonwoven fabric; all the carrier fabrics were made of polyester. The woven fabrics were provided by Engelbert E. Stieger (Rorschacherberg, Switzerland) and the nonwoven fabrics by Fritz Landolt AG (Näfels, Switzerland). The woven textile sample was used as a carrier fabric for two different stitching patterns ('M' and 'V') as presented in Fig. 3. To obtain such embroidery, the optical fibers had to be fixed with a certain amount of fixation points with the carrier textile (marked in red in Fig. 3). As can be seen in Fig. 3, the shape 'M' had 9 fixation points comparing to 5 fixation points in the 'V' shape pattern. The entire sample with 'V' pattern consisted of 82 optical fibers and the sample with the 'M' pattern was made of 54 optical fibers.

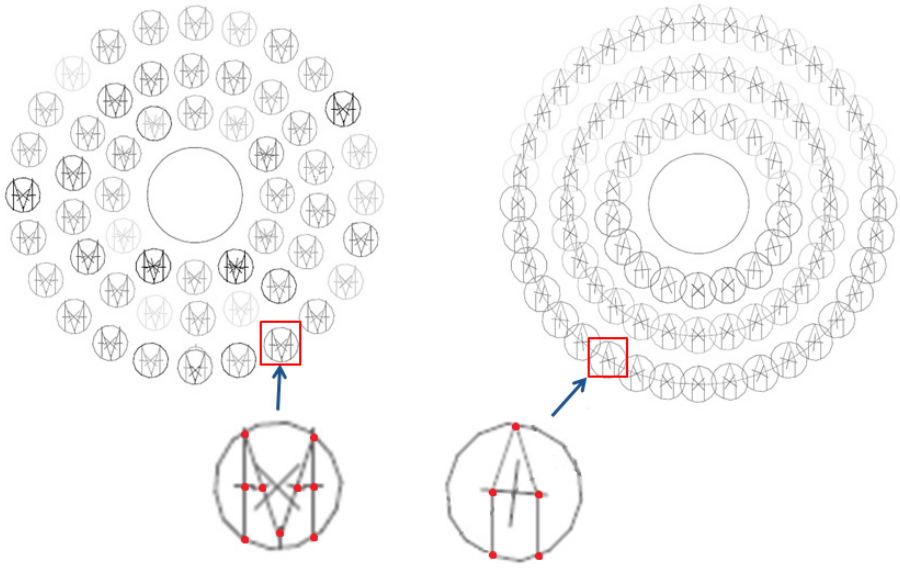

Fig. 3. Two types of embroidery patterns. On the left hand side, the 'M' type pattern is presented and on the right hand side, the 'V' type pattern. Red dots represent fixation points with the carrier textile. Pattern 'M' consisted of 54 optical fibers (12, 18, 24 in each ring from the middle to the outer one, respectively) whereas total number of fibers in the ' V' pattern was 82 (18, 28, 36 in each ring counting from the middle to the outer one)

The samples with the 'V' pattern were produced four times and underwent the following surface modifications: (1) cladding removal by rubbing the sample with a cloth immersed with solvent (acetone), (2) surface roughening by scratching with diamond lapping paper (3

#211135 - $15.00 USD Received 29 Apr 2014; revised 7 Jun 2014; accepted 8 Jun 2014; published 9 Jul 2014

µm grit) and (3) addition of polydimethylsiloxane (PDMS) layer on top of the samples. The PDMS was a Silicone Elastomer Kit (Sylgard® 184) provided by Dow Corning. It consisted of PDMS in a liquid form and a curing agent. Once mixed, it was placed in a desiccator and dried *in vacuo*. Afterwards the PDMS mixture was smeared over the sample forming a 1 mm thick layer. A summary of the produced samples with their abbreviated entries are presented in Table 1.

Table 1. Listing of all manufactured samples and their abbreviations

Fiber type	Carrier fabric	Abbreviation
738* [‘V’ pattern]	Woven fabric	V_WV
738 [‘M’ pattern]		M_WV
738 [‘V’ pattern]	Thick nonwoven	V_TCK
	Thin nonwoven	V_THN
738 [removed cladding]		RC_WV
738 [surface roughened]	Woven fabric	SR_WV

*Fiber code name, core Zeonor, cladding THV. More details in [20].

2.3 Measurement of the light coupling efficiency

In Fig. 4, the measurement setup of the in-coupled light efficiency is shown. A human tissue model was made of PDMS with the addition of Indian ink for light scattering purposes as described in [29]. The setup consisted of a PCB board with an LED (570 nm) placed in the center of the board, a metal ring for supporting the PDMS-based human tissue model covering the metal ring and the LED (as presented in Fig. 4(a)). Figure 4(b) shows the way the textiles were placed on the optical tissue model when tested. The bundled fibers from each ring were combined and glued with a fiber optic epoxy glue (F112) into an SMA 905 connectors both provided by Thorlabs GmbH (Dachau/Munich, Germany). In order to achieve flat fiber facets for good light coupling efficiency, the fiber bundles were polished with diamond lapping films (in this order: 6 µm, 3 µm and 1 µm grit) after the glue was dried (24 h at room temperature). The collected light was analyzed using a photomultiplier (PMT) provided by PRC Krochmann GmbH (Berlin, Germany) combined with an integrating sphere. Measurements of light coupling efficiency were conducted five times.

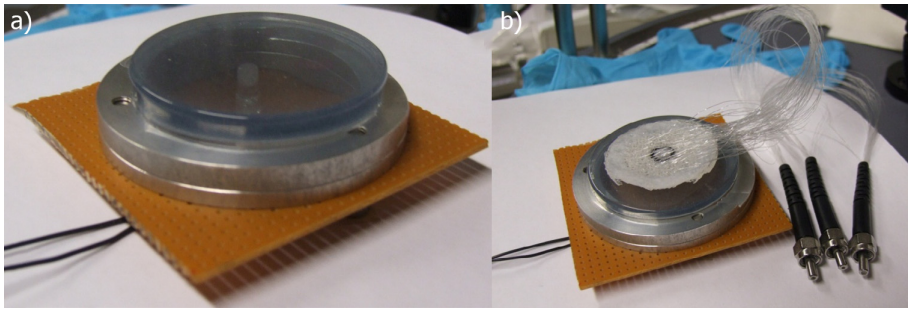

Fig. 4. Setup for measurements of the light in-coupling efficiency. On (a) the setup of the PDMS-based human tissue model is shown. The PDMS consisted of India ink and the polymer film was placed on the supporting metal rings and the LED was located centrally. (b) shows the placement of the textile when tested

2.5 Heart rate and oxygen saturation measurements (SpO2)

The pulse wave signals were analyzed with a near infrared tissue spectrometer Oxiplex provided by ISS (Champaign, USA), the same apparatus providing the light sources. This tissue spectrometer consists of laser diodes (with emitting peaks at 692 nm and 834 nm and power 5 mW each) that acts as light sources and photomultiplier tubes (PMT) for light

#211135 - $15.00 USD Received 29 Apr 2014; revised 7 Jun 2014; accepted 8 Jun 2014; published 9 Jul 2014

detecting purposes. The light sources are time multiplex for measurements. The tests were performed with the fabric V_WV (Table 1), which was located on the middle finger of the right hand, as presented in Fig. 5. First, fibers from all the rings were combined and placed into the light detecting part of the Oxiplex. In a second measurement, the signal from the fiber bundles from each ring was characterized separately.

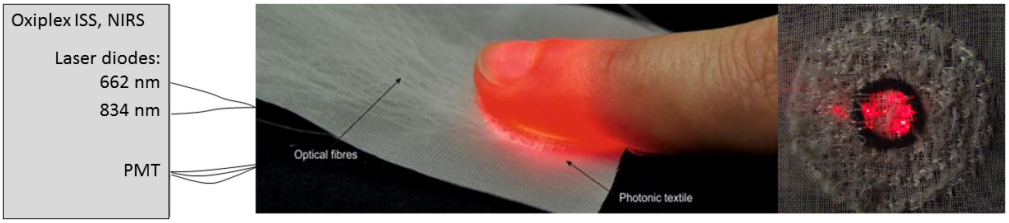

Fig. 5. Measurement conditions of the heart rate and the oxygen saturation recording using the presented photonic textile. Light is coupled from the middle of the textile into the tissue of the finger and is then scattered back to the textile. On the right hand side top view of the photonic textile, without the finger, is presented: light is delivered by the central fiber, while the black ring prevents "short circuit" (see also Fig. 2).

The oxygen saturation was calculated using the modified Beer-Lambert law. According to this law, following equations were solved to obtain changes in oxygenated (O2Hb) and deoxygenated (HHb) haemoglobin [9]:

$$\Delta HHb \times d \times DPF = (-0.239\Delta A_{692nm} + 0.099\Delta A_{834nm})$$

$$\Delta O_2Hb \times d \times DPF = (0.185\Delta A_{692nm} - 0.508\Delta_{834nm})$$

where ΔA692nm and ΔA834nm are the amplitudes of the light attenuations caused by the pulsation, d is the distance between illuminating and detecting point and DPF the differential patch length factor, which occurs in tissue due to multiple scattering. Factors d and DPF were assumed to be the same for both wavelengths. Since the arterial oxygen saturation is determined by the ratio ΔO2Hb/(ΔO2Hb + ΔHHb), d and DPF cancel. Thus the following equation was used for the SpO2 calculations [9]:

$$SpO_2[\%] = \Delta OHb / (\Delta O_2Hb + \Delta HHb)$$

All data were recorded from one human subject in a resting position. Furthermore, for cross comparison, the measurements were compared with a measurement performed with a commercial system Nellcor N-395 provided by the University Hospital Zürich.

All the recorded data were imported into MATLAB R2012b for further signal processing. Bandpass filtering between 0.5 and 2.5 Hz was applied in order to minimize movement artefacts and other noises. After the filters were applied, recorded data were used to calculate the SpO2 values according to the description in paragraph 2.4. To extract the frequency of the heart rate, a Fourier transformation was performed. Heart rates and SpO2 results were smoothed with moving average algorithms.

3. Results and discussion

3.1 Wearable long-term monitoring system

In order to maintain a good wearing comfort, which is needed for the long term monitoring, these medical textiles should be highly flexible. This allows the adaption of the textile patch to any complex body surface. The amount of fixation points of the embroidery influences the drapability of the fabric. A higher amount of this fixation points facilitate the production process, but on the other hand enhance the rigidity of the fabric. The 'M' shape embroidery pattern consisted of 9 fixation points while the 'V' shape pattern had only 5 fixation points (Fig. 3). The total amount of fixation points per sensor was therefore 486 for the 'M' type sample and 410 for the 'V' type sample.

#211135 - $15.00 USD Received 29 Apr 2014; revised 7 Jun 2014; accepted 8 Jun 2014; published 9 Jul 2014

In Fig. 6, the flexibility of the textile is demonstrated. In order to determine whether the embroidered fibers out-coupled the light efficiently, and if the rings were well separated, the bundled optical fibers from each light-collecting ring were connected to a light source of a different color. As can be seen from the image, the rings were well separated and light was out-coupled from the bends of the embroidered fibers. Furthermore, the three dimensional black ring prevented a light sort circuit from the out-coupled light of the outer rings to the optical fibers embroidered in the center of the ring system. Such a short circuit would dramatically decrease the light pulsation amplitude, a parameter which has to be maintained as high as possible for measurements in pulse oximetry devices.

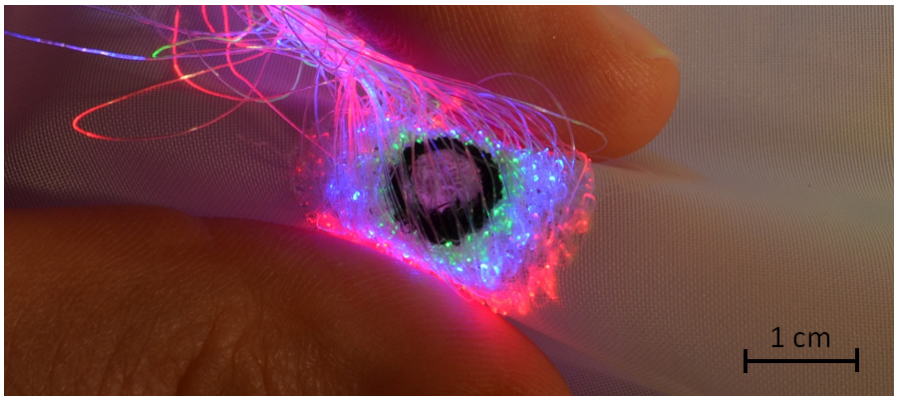

Fig. 6. A luminous textile used in this study is bent to show the flexibility of the fabric. The fiber bundles of each ring were connected to LEDs with different colours to illustrate the successful separation of the fiber bundles and the light out-coupling efficiency.

3.2 Efficiency of light in-coupling

To obtain a maximal signal to noise ratio, we determined, which sample has the highest light in-coupling efficiency. The measurements were conducted using the setup illustrated in Fig. 4.

Firstly, the influence of the stitching pattern (‘M’ and ‘V’) was evaluated. The light in-coupling efficiency for the optical fibers embroidered in a ‘V’ shape was 35% higher than when embroidered in an ‘M’ pattern. The reason lies in the enhanced number of ‘V’s being stitched in the patch compared with the ‘M’s: with the ‘V’ pattern 82 fibers could be stitched into the carrier fabric whereas for the ‘M’ patterned sample only 54 fibers fitted in the same textile area. This effect over-compensated the launching efficiency of the increased in-coupling points of the ‘M’ pattern.

In the next step, the effects of carrier fabrics were assessed. Due to the higher rigidity of the fabrics with the ‘M’ pattern and the decreased efficiency, the fabric tests were performed with the optical fibers embroidered in a ‘V’ shape. As can be seen from Fig. 7, the matrix fabric, which led to the highest efficiency was the woven fabric. Nonwoven fabrics have a much higher yarn density than the woven fabric. As a consequence, the fabric material absorbed more of the out-coupled light.

Lastly, the surface modification of the optical fibers in order to enhance the coupling efficiency was assessed. As it can be noticed from Fig. 7, none of the studied surface modifications increased the efficiency. The first idea was to remove the cladding from the fibers in the area where the textile would be in touch with the tissue. A higher efficiency was expected due to direct optical contact of the fiber’s core with the tissue. However, fabric RC_WV had a light coupling efficiency, which was 63% lower than the untreated patch V_WV. The cladding of the optical fibers was removed by applying a mechanical force in the presence of organic solvent (acetone). The cladding material THV is well soluble in acetone whereas the Zeonor core material is not [solubility information was provided by manufacturers of the polymers]. It was empirically proven that this solvent did not dissolve

#211135 - $15.00 USD Received 29 Apr 2014; revised 7 Jun 2014; accepted 8 Jun 2014; published 9 Jul 2014

the polymer of the core. However, this treatment negatively influenced the light transmission parameters.

Roughening the surface (SR_WV), which mainly consisted in producing big numbers of micro cracks and ditches that would act as light coupling areas, decreased the efficiency by nearly 75% compared to the most efficient non-treated fabric V_WV.

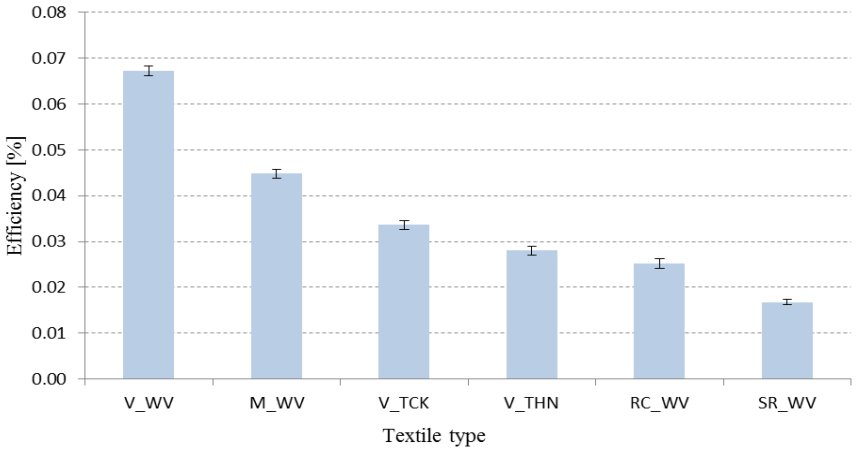

Fig. 7. Efficiency of light coupling into photonic textile with its standard deviation (n = 5)

3.4 Measurements of pulse waves and of the oxygen saturation

In Fig. 8, time traces, without any signal processing, of light absorbed in the tissue together with calculated heart rate and blood oxygenation are shown. Parts (a), (b), and (c) represents data acquired from each individual ring (first, second and third ring respectively, counting from the center of the ring system as illustrated in Fig. 2). The measured data were compared with the data obtained from a commercial Nellcor sensing system. The oxygen saturation levels for all measurements were in the range of 92-98%, which are expected values for healthy human beings [30]. The biggest deviation between the commercial Nellcor sensing system and the proposed sensor were detected in the SpO2 measurement (a). In the first 15 seconds of this measurement a miscorrelation of results of up to 5% (92% for textile based system and 97% for commercial device) was observed. This miscorrelation were also observed for the recorded pulse. This effect can be explained by a low signal to noise ratio, which is due to the small amount of optical fibers (18) collecting light in the first ring. After about 15 seconds of this measurement the data correlated better and eventually showed a very good correlation (less than 1% deviation). However, the obtained heart rate values from the two instruments correlated much better. Fewer artefacts were observed in measurement (b), from the middle ring (ring 4 in Fig. 2) where 28 optical fibers were collecting light. During the first 10 seconds, signal from proposed textile system underestimated the SpO_2 value by 2% during which a lot of noise was present. Pulse data correlated well however, between 15 and 20 seconds, an increased deviation of 7 heart beats per minute was observed. As for the measurements of the first two rings, for ring 4 (measurement c) an enhanced amount of noise was present at the beginning of the measurement, which prevented the determination of the SpO2 value during the first 5 seconds. For measurements (c) and (d) the variation of the SpO2 signal was below 1%. For these measurements more optical fibers were used (36 optical fibers for (c) scenario and 82 for (d) where all three rings were combined for launching the light), which underlines the fact that the more optical fibers are used the better accuracy can be obtained. Reasonable agreement was obtained for the values collected from rings b), c) and d).

#211135 - $15.00 USD Received 29 Apr 2014; revised 7 Jun 2014; accepted 8 Jun 2014; published 9 Jul 2014

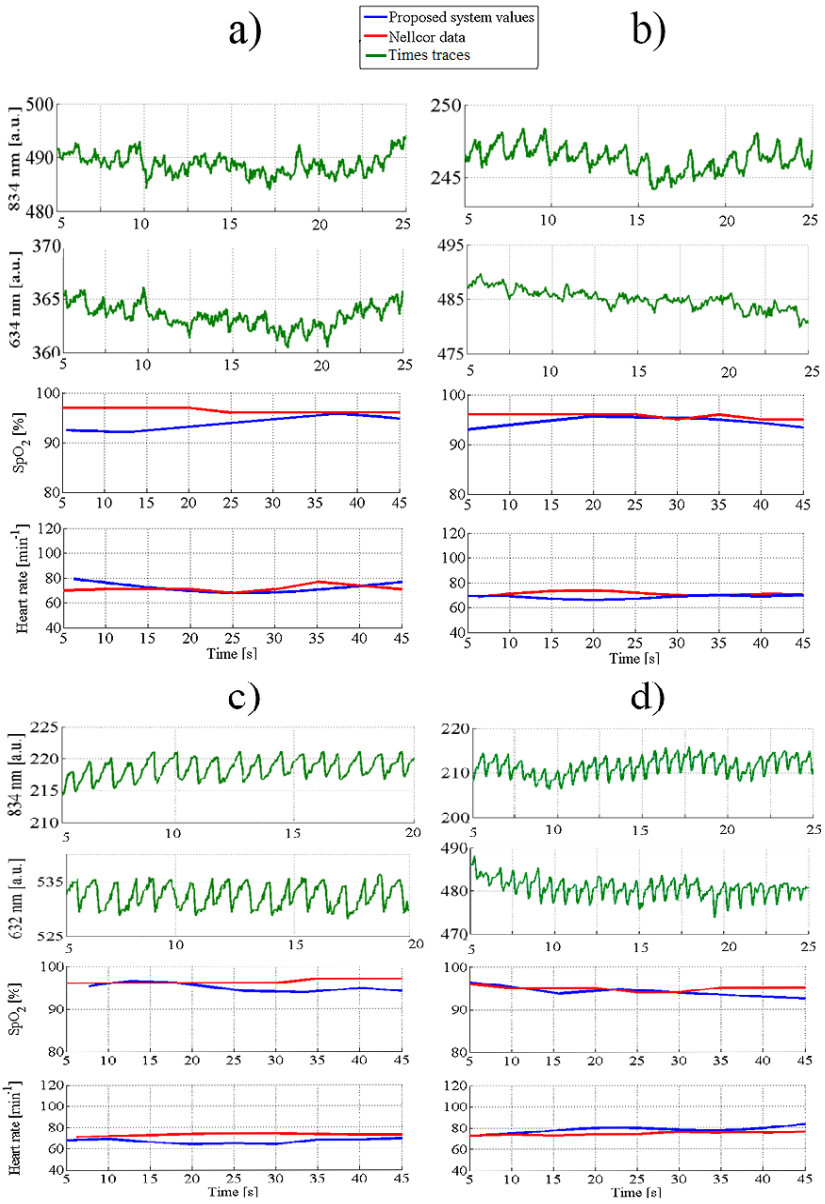

Fig. 8. Graphs presenting the original time traces of light absorption in the tissue together with the calculated heart rate and blood oxygenation values. Parts (a), (b) and (c) represent measurements form rings 2-4 (Fig. 2) respectively; and in (d) the fibers of all three rings were combined.

4. Conclusions

In this paper, a fully textile-based pulse-oximeter was presented. This photonic textile work in reflection mode, which makes them very versatile for wearable long-term monitoring and allow the measurements in different parts of the body like forehead, chest, arms, etc. Furthermore, the presented fabric has the haptic of conventional fabrics and thus enhances the acceptance of the wearer, which is necessary for long-term monitoring purposes. The data were additionally crossed compared with commercial device and showed good correlation once enough fibers were used to collect the outcoupled light.

#211135 - $15.00 USD Received 29 Apr 2014; revised 7 Jun 2014; accepted 8 Jun 2014; published 9 Jul 2014

The same principle can be used for near-infrared spectroscopy to monitor the perfusion in the tissue. This is of great importance to monitor the perfusion to detect decubitus as early as possible, and where flexible textile-based sensor solutions are required. Further work implies the miniaturization of the electronic components to obtain a fully wearable sensing system.

Acknowledgments

This work was financially supported by NanoTera (TecInTex). Gratefully acknowledged is the support of Michel Schmid, Joanna Frackiewicz Kaczmarek and the valuable scientific discussions with Damien Ferrario and Josep Solà.

#211135 - $15.00 USD Received 29 Apr 2014; revised 7 Jun 2014; accepted 8 Jun 2014; published 9 Jul 2014